UDK 628.336:54-126:21.315.222
Original scientific article/Izvirni znanstveni članek

ISSN 1580-2949
Mater. Tehnol.

INFLUENCE OF CURING STRESS ON THE PULL-OUT BEHAVIOR OF A SINGLE GEOGRID RIB PLACED IN CEMENT-STABILIZED DREDGED SLURRY

VPLIV UTRJEVALNE NAPETOSTI NA MEHANSKO OBNAŠANJE S KOVINSKO MREŽO OJAČANEGA IN S CEMENTOM STABILIZIRANEGA REČNEGA BLATA

Chengchun Qiu*, Liwei Xu, Yang Li, Dan Zhang

School of Civil Engineering, Yancheng Institute of Technology, Yancheng 224051, Jiangsu Province, China

Prejem rokopisa – received: 2025-07-03; sprejem za objavo – accepted for publication: 2025-10-07

doi:10.17222/mit.2025.1515

Cement-stabilized dredged slurry, despite its enhanced compressive strength, lacks tensile strength, particularly with low cement contents. Geogrid reinforcement is usually used in high-fill projects to improve the soil tensile and shear strengths, but research on their interface characteristics under curing stresses is limited. A prior understanding of the frictional properties at the interface is crucial for assessing the impact of curing stress on the interface property of geogrid-reinforced cement-stabilized slurry, given the geogrid mesh's intricate interlocking. The study included pull-out tests on cement-stabilized dredged slurry reinforced with a single geogrid rib, after removing the mesh openings. The results showed that regardless of whether the curing stress was applied, the pull-out curves showed that the pull-out force increased rapidly in the initial stage and then gradually decreased after reaching the peak force. Specimens that had undergone curing stress exhibited consistently higher peak pull-out forces compared to those that had not. The interfacial shear strength increased with the normal stress, with reduced moisture content and increased cement dosage correlating with elevated shear strength. Higher moisture content significantly reduced interfacial cohesion, with a slight increase in the friction angle. Conversely, increased cement content significantly raised both interfacial cohesion and friction angle. Curing stress primarily affected the interfacial cohesion, with a relatively minor impact on the friction angle.

Keywords: dredged slurry, geogrid, curing stress, interface properties, pull-out test

S cementom stabilizirana gošča ali mulj z rečnega ali morskega dna kljub temu, da ima dokaj dobro tlačno trdnost, ima zelo slabo natezno trdnost, če je stabilizirana z majhno vsebnostjo cementa. Zato se jo običajno armira še s polimerno mrežo v primeru projektov z veliko polnitvijo materiala in, kjer se zahteva dobra natezna in strižna trdnost zemljine. Pretekle raziskave so pokazale, da ima zemljina kljub tem ukrepom oslabljene medfazne karakteristike zaradi napetosti, ki nastanejo med njenim utrjevanjem oziroma strjevanjem. Razumevanje lastnosti zemljine zaradi trenja, ki nastaja na mejah med posameznimi sestavinami (fazami) je ključnega pomena za oceno vpliva napetosti nastalih med strjevanjem z geomrežo armirane in s cementom stabilizirane gošče, glede na zapleteno prepletanje geomreže. V tej študiji so avtorji izvedli mehanske teste izvlačenja (angl.: pull-out tests) na s cementom stabilizirani gošči armirani z geomrežo. Preizkus izvlačenja se običajno uporablja za testiranje betona (ali utrjene zemljine) pri katerem merimo silo s katero poizkušamo in vzorca utrjenega materiala potegniti palico izbrane oblike in velikosti, ki je bila predhodno ulita vanj. Rezultati analiz so pokazali, da je kljub nastanku napetosti zaradi utrjevanja materiala na krivuljah izvlačenja prišlo v začetnem stadiju obremenjevanja najprej do hitrega naraščanja sile potrebne za izvlačenje palice in nato do njenega postopnega zmanjševanja po dosegu vršne (maksimalne) vrednosti sile. Pri preizkušancih, ki so bili izpostavljeni napetostim zaradi strjevanja so avtorji izmerili višje vrednosti maksimalne sile izvlačenja, kot tisti, ki niso bili izpostavljeni le-tem. Medfazna strižna trdnost je naraščala z normalno napetostjo pri zmanjšani vsebnosti vlage in povečani vsebnosti cementa. Ustrezno se je povečevala tudi strižna trdnost preizkušancev. Pri višji vsebnosti vlage se je znatno zmanjšala medfazna kohezija pri rahlem povečanju notranjega kota trenja (angl.: friction angle). To je veličina, ki opredeljuje sposobnost materiala za prenašanje strižnih napetosti (obremenitev). Nasprotno pa je povečana vsebnost cementa znatno povečala tako medfazno kohezijo kot tudi notranji kot trenja. Napetosti nastale zaradi strjevanja v glavnem vplivajo na medfazno kohezijo z relativno majhnim vplivom na notranji kot trenja.

Ključne besede: rečno ali morsko blato (mulj), polimerna mreža za armiranje (geomreža), utrjevalna napetost, medmejne lastnosti, preizkus izvlečenja

1 INTRODUCTION

With the acceleration of urbanization and the development of waterway transport engineering, large quantities of slurry are dredged from harbors, navigation channels, and reservoirs.[1–3] Annually, hundreds of millions of cubic meters of sediments are dredged worldwide.[4] For instance, over 100 million cubic meters of slurry are dredged from Chinese ports and waterways each year. Due to its high initial water content, often exceeding two to three times the liquid limit, this dredged slurry exhibits low strength and poor engineering properties, rendering it unsuitable for direct use in construction projects.[5,6] If not properly treated and utilized, this type of slurry can cause environmental pollution and ecological damage.[7]

*Corresponding author's e-mail:
craigqiu@163.com (Chengchun Qiu)

In the context of dredged slurry management, conventional treatment strategies predominantly rely on dewatering and solidification processes. Dewatering techniques, while widely employed, tend to be both time-consuming and labor-intensive, often impeding the progress of construction projects. As an alternative, the conversion of dredged slurry into a usable fill material through solidification represents a common and effective approach to resource utilization. This process typically involves the use of curing agents such as cement, lime, mineral powder, or fly ash.[8,9] These agents engage in various chemical reactions with the water in the slurry, leading to a reduction in water content and the formation of hydration products that enhance the strength of the cement-stabilized slurry.[10,11] The resulting cement-stabilized dredged slurry finds extensive application in civil engineering projects, including its use as a road subbase or embankment fill, and as backfill material for retaining walls. This not only minimizes the environmental impact by reducing land use for disposal but also provides economic benefits through the repurposing of dredged materials.

In the practice of engineering construction, geogrids, as an economical and efficient reinforcing material, are widely embedded within various fillers to enhance the stability and bearing capacity of composite soil bodies. Their low cost and ease of installation have led to their extensive application in soil slope stabilization, roadbed construction, retaining walls, and other reinforced soil structures.[12–14] Although cement-stabilized dredged slurry, due to the adhesive action of cement hydration products, exhibits higher compressive strength compared to natural soil, its tensile strength remains significantly lower. In response to this issue, in high-fill projects, it is often necessary to combine geogrid reinforcement techniques to enhance the tensile and shear strengths of composite soil bodies. In retaining wall projects, cement-stabilized soil can be used as the wall, and geogrids can be placed in layers in both the cement-stabilized soil and the fill material; the geogrids are placed directly in the cement-soil mixture, which is then allowed to set and take shape without additional installation. This structural design is not only cost-effective but also very stable.[15] In the design of reinforced soil, the interface characteristics between geogrids and fillers are of crucial importance. Numerous studies have shown that soil type, moisture content, geogrid type (such as mesh size, strength, etc.), and boundary conditions significantly influence interface characteristics.[16–19] However, research on the interface characteristics of geogrids and cement-stabilized soil is still limited,[3] especially regarding the effects of the normal pressure generated by fill-in high-fill projects on the curing of cement-stabilized soil.[20] The impact of this curing stress on the interface characteristics is rarely studied and merits further investigation. In existing research on interface characteristics of reinforced soil, geogrids are typically treated as an equivalent surface for analysis, incorporating both the interface friction effects and the interlocking effects of the geogrid mesh. Nevertheless, to accurately reflect the influence of curing stress on the interface characteristics of geogrid-reinforced cement-stabilized soil, it is first necessary to clarify the friction characteristics of the interface between the geogrid reinforcement and the cement-stabilized soil.

This study exclusively considered the interface friction effects by conducting a series of pull-out tests to analyze the interface properties of a single-rib geogrid embedded within the cement-stabilized dredged slurry. To discern the impact of variations in water content and cement concentration, cement-stabilized dredged slurry samples were systematically prepared with three distinct initial water contents and three diverse cement contents, encompassing both cured and uncured conditions under stress. During the pull-out tests, three different normal pressures were applied to evaluate the influence of curing stress, moisture content, cement content, and normal pressure on the interface properties. The outcomes were methodically assessed by examining pull-out curves, and interface shear strength parameters.

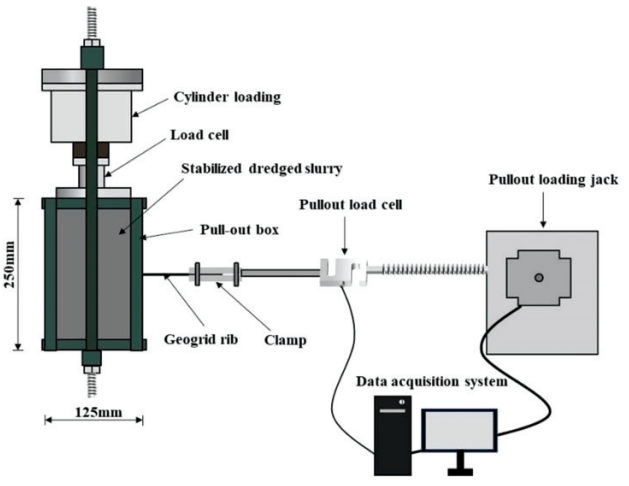

Figure 1: Pull-out test equipment

2 EXPERIMENTAL PART

2.1 Test instruments

All tests in this study were conducted using a custom-built pull-out test device, shown in **Figure 1**. The apparatus consists of a pull-out box, a horizontal loading device, a vertical loading device, load cells, and potentiometers. The internal dimensions of the pull-out box were (125 × 125 × 250) mm.[3] Transparent acrylic panels, 10-mm thick, were installed on all four sides of the pull-out box to allow for observation of specimen deformation during the test. Vertical and horizontal loads were applied using an electric motor and a pneumatic system. The displacement of a single rib of the geogrid during the pull-out test was measured using a potentiometer, while the pull-out load was recorded by a load cell with a maximum range of 10 kN. A digital controller captured

both the applied pull-out force and the corresponding displacement.

2.2 Materials

2.2.1 Dredged slurry and cement

The dredged slurry samples were collected from a dredging site in Funing County, Yancheng City, China.[3] The slurry was initially air-dried, then crushed and sieved through a 2-mm screen. The processed soil was further dried and stored for use in the experiments. **Table 1** presents the basic physical properties of the Funing soil, which had a liquid limit of 52 % and a plastic limit of 23.5 %. According to the Unified Soil Classification System (USCS), the Funing soil was classified as high-plasticity clay. The curing agent used in this study was ordinary silicate cement (42.5 R/N), supplied by Jianing Cement Co. in China.

Table 1: Basic physical properties and clay mineral content of Funing soil

	Physical property index	Values
	Liquid limit/%	52
	Plastic limit/%	23.5
	G_s	2.7
Amounts of different particle sizes/%	Sand/% (d > 0.005 mm)	4.0
	Silt/% (0.005–0.075 mm)	80.7
	Clay/% (d < 0.005 mm)	15.3

2.2.2 Geogrid

Due to strong cohesion between the particles of the cement-stabilized slurry, the selection of a high-strength geogrid is necessary to ensure the geogrid rib is pulled out rather than broken, thus facilitating a clear analysis of the interfacial behavior. The geogrid utilized in the tests was a standard biaxial plastic geogrid, characterized by a longitudinal mean tensile strength of 50 kN/m. Before the experimentation, an individual longitudinal geogrid rib was fabricated by trimming the transverse ribs of the biaxial geogrid, as shown in **Figure 2**. The terminal segments of the transverse ribs were retained for fixation with the clamps, ensuring that the single rib of the geogrid maintained a substantial tensile strength at the clamp position during the pull-out process. **Table 2** presents the physical and mechanical parameters of the geogrid. The effective size of the single rib buried in the slurry was (110 × 2.5) mm (length × width).

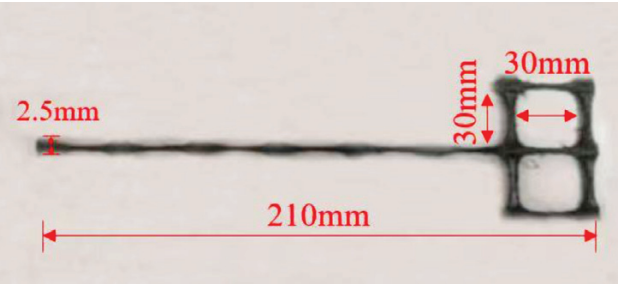

Figure 2: Geogrid single rib

Table 2: Performance parameters of the geogrid

Characteristic	Values
Type	TGSG5050
Aperture size (mm)	30 * 30
Longitudinal mean strength (kN/m)	≥50
Longitudinal strength at 2-% strain (kN/m)	≥17
Longitudinal strength at 5-% strain (kN/m)	≥34

2.3 Test program

The water content of the pull-out test sample was set at (78.2, 104.3 and 130.1) %, corresponding to 1.5, 2, and 2.5 times the liquid limit, respectively. The cement content was defined as the weight of cement per cubic meter of wet dredged slurry, with values of (50, 100, and 150) kg/m^3, respectively.[3]

The preparation of the specimens was carried out through a defined sequence of actions: Initially, cement was combined with dredged slurry and incrementally filled into the pull-out box with the assistance of a mixer, layer by layer, until the midpoint of the box was achieved. Subsequently, a single rib of the geogrid was positioned within the box. Following the placement of the geogrid rib, the cement-slurry blend was further introduced into the box to attain the target height. The assembled model box was then transferred to a controlled-environment room, and maintained at a steady temperature of 20 ± 2 °C, where it was allowed to cure for 28 d.

Depending on the specific requirements of each specimen, the curing process was conducted under either stressed or unstressed conditions. The application of curing stress was omitted during the early curing phase due to the elevated moisture content in the dredged slurry and the limited initial strength of the cement matrix. As a result, curing stress was not imposed during the initial 7-day period. Starting from the 7th day up to the 14th day, a curing stress of 200 kPa was introduced, which was then increased to 400 kPa after the 14th day and maintained until the conclusion of the curing period on the 28th day.

A series of pull-out tests were conducted to analyze the behavior of the geogrid rib embedded in cement-stabilized dredged slurry. **Figure 3** depicts the procedural flow of the experiment. The experimental variables included different water contents, cement contents, and normal pressures. The pull-out tests were performed at a displacement rate of 1 mm/min and were terminated when the pull-out force either peaked and then sharply decreased or stabilized. Test conditions are detailed in **Table 3**.

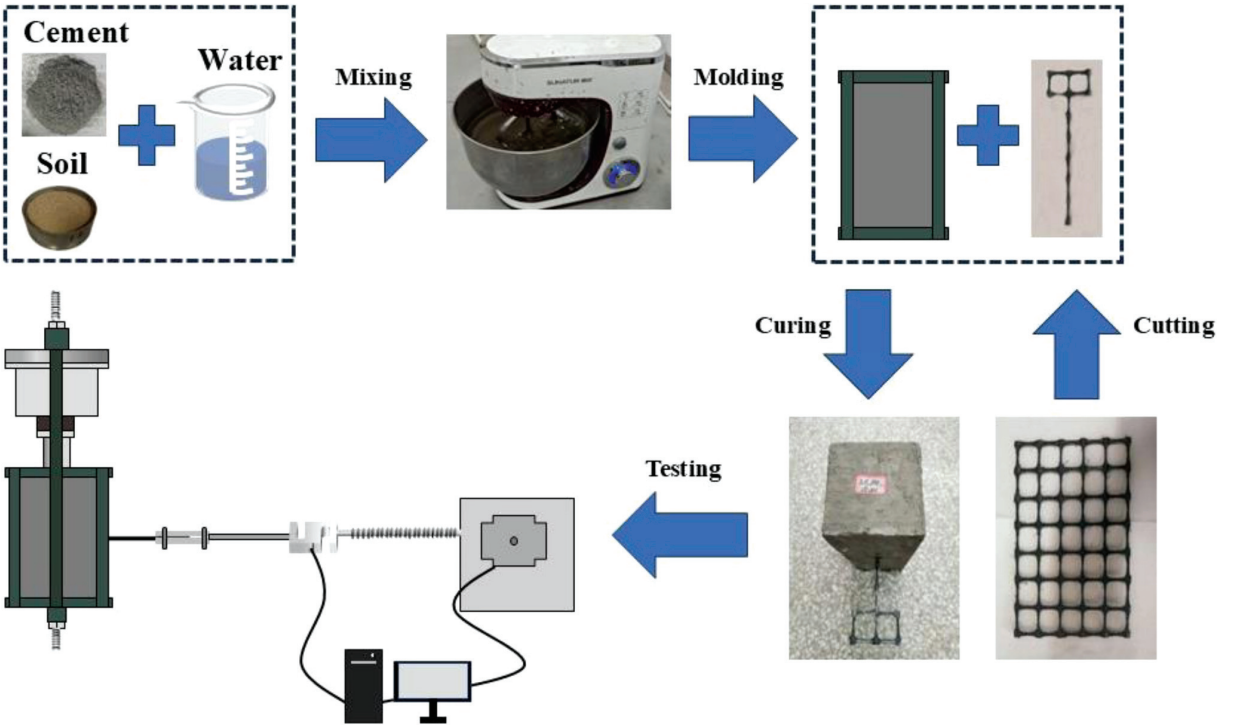

Figure 3: Test flow chart

Table 3: Pull-out test cases

Water content w (%)	Cement dosage C (kg/m^3)	Curing time t (days)	Normal pressure σ (kPa)	Curing stress P (kPa)
78.2	100	28	50/100/150	0–7 d: 0
104.3	50/100/150			7–14 d: 0/200
130.1	100			14–28 d: 0/400

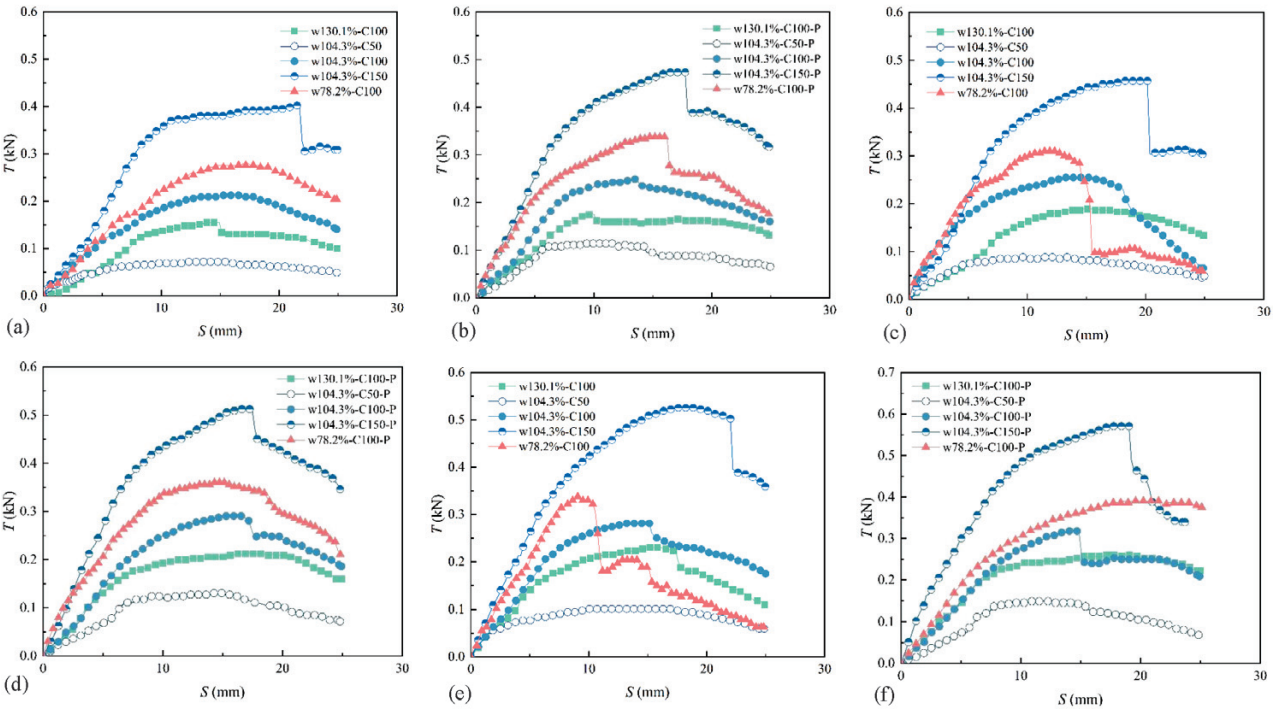

Figure 4: Pull-out force against displacement for varied test setups at normal pressures of: a) 50 kPa, c) 100 kPa, e) 150 kPa in the absence of curing stress, as well as b) 50 kPa-P, d) 100 kPa-P, f) 150 kPa-P in the presence of curing stress

3 RESULTS

3.1 Pull-out force-displacement performance

Figure 4 illustrates the relationship between pull-out force (T) and displacement (S) under various test conditions, both with and without curing stress and across different normal pressures. In the legend of **Figure 4** and all subsequent figures, P indicates that the specimen was subjected to curing stress. The curves depicting pull-out force versus displacement exhibit similar shapes under identical test conditions. Initially, for all specimens, the pull-out force increases rapidly with increasing pull-out displacement, indicating that the single rib of the geogrid demonstrates a force mechanism for rapid mobilization of the pull-out force during the extraction from the stabilized dredged slurry. As displacement continues to increase, the pull-out force mobilized along the geogrid's single rib persists, but the growth rate gradually decreases. Ultimately, the curve reaches a significant peak pull-out force before displaying a slower decline, consistent with the experimental findings of Qiu et al. (2024).[3] Additionally, the peak pull-out force of specimens with the same moisture content and cement admixture increases with higher normal pressure. This is due to the elevated normal pressure exerting greater pressure on the soil body, leading to increased compaction between the soil and the geogrid's single rib, thus enhancing the pull-out force during the extraction process. It is evident that, for the same normal pressure and cement content, the rate of increase in the pull-out force-displacement curve for the specimens with lower water content is greater than that for the specimens with higher water content. Increased water content reduces the pull-out force required to achieve the same displacement. Furthermore, the pull-out curves of the specimens with high cement content surpass those of the specimens with low cement content under the same normal pressure and water content, indicating that a higher cement content necessitates a greater pull-out force to reach the same displacement.

Notably, in **Figure 4**, some curves exhibit a sudden drop. This phenomenon predominantly occurs in the samples with low moisture content or high cement content. Under these conditions, the brittleness of the samples increases. As the geogrid rib is progressively pulled out under the action of the pull-out force, cracks at the interface between the rib and the cement-stabilized slurry begin to form. An increase in brittleness accelerates the development of these cracks, resulting in a corresponding decline in the pull-out force.

Figure 5 compares the pull-out force-displacement curves of specimens with and without curing stress under various normal pressures. The specimens exhibiting the same moisture and cement content demonstrated a faster growth rate and higher peak pull-out force with increasing normal pressure. For a given normal pressure, the peak pull-out force of the specimens subjected to curing stress exceeded that of the specimens without curing stress. This enhancement was attributed to a greater internal compaction of specimens under the curing stress

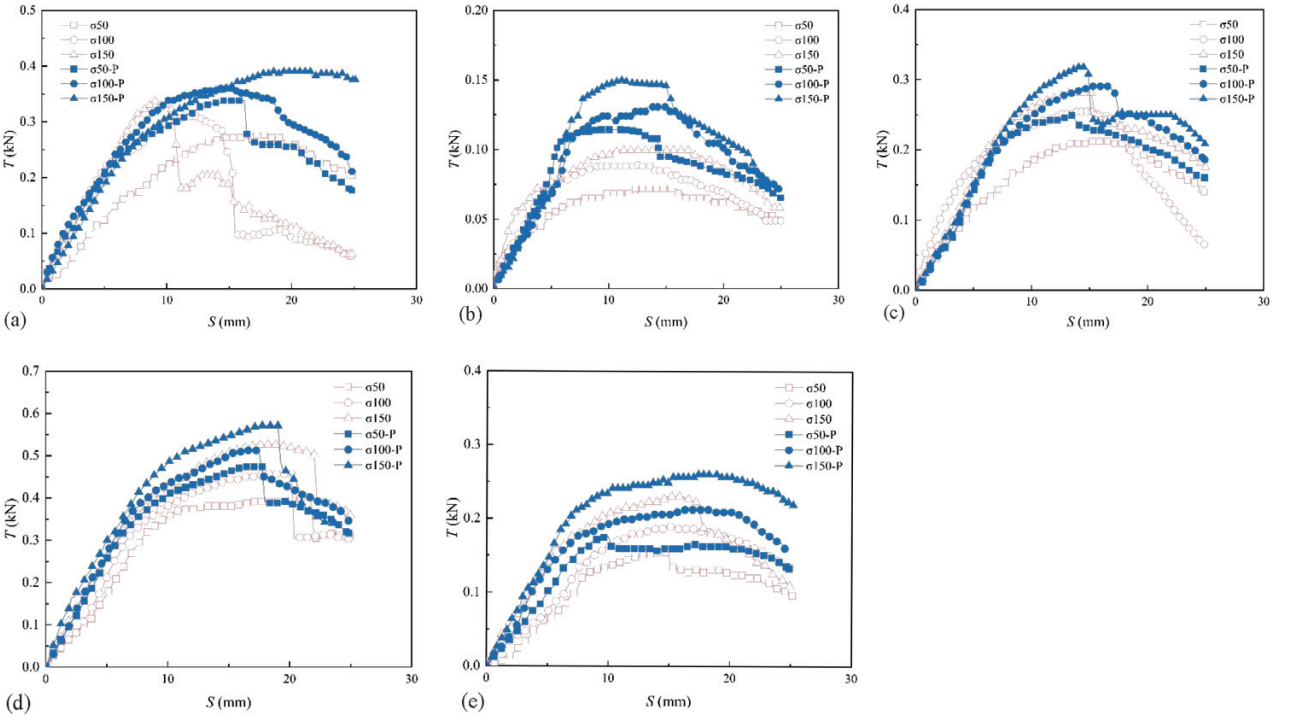

Figure 5: Pull-out force-displacement plots for specimens subjected to varying normal pressures with and without curing stress, categorized by water-cement ratios and cement densities as follows: a) w = 78.2 %, C = 100 kg/m^3, b) w = 104.3 %, C = 50 kg/m^3, c) w = 104.3 %, C = 100 kg/m^3, d) w = 104.3 %, C = 150 kg/m^3, e) w = 130.1 %, C = 100 kg/m^3

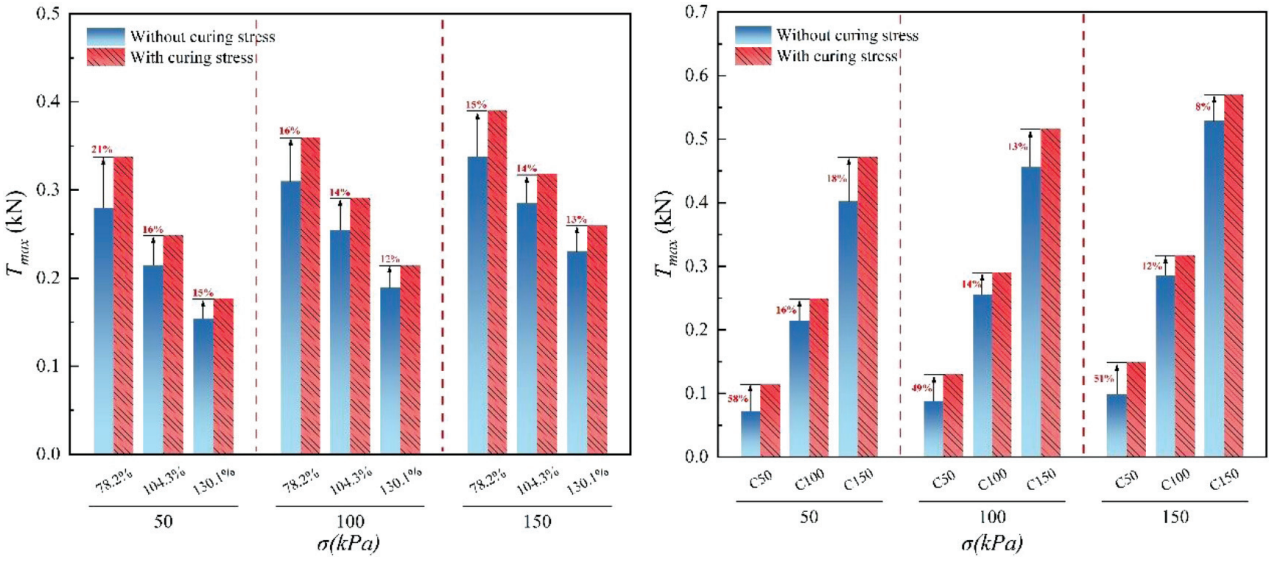

Figure 6: Comparison of maximum pull-out forces with and without curing stress at different normal stresses: a) under different moisture contents, b) under different cement contents

during the curing stage, resulting in a stronger bond between the soil and the ribs. This phenomenon was particularly pronounced in the specimens with a moisture content of 104.3 % and a cement content of 50 kg/m^3. Conversely, in the specimens with a moisture content of 104.3 % and a cement content of 150 kg/m^3, the effect of curing stress was minimal, leading to curves that are relatively close to each other, as illustrated in **Figure 5d**. This phenomenon was consistent with the experimental results of Qiu et al. (2024).[3]

Furthermore, as illustrated in **Figures 5a** to **5c** and **5e**, the application of curing stress enhanced the pull-out force of the specimens at a specific normal pressure, approaching the pull-out force of the specimens without curing stress at the subsequent level of normal pressure. For instance, for the specimen with a moisture content of 104.3 % and a cement content of 100 kg/m^3, the curve under a curing stress of 100 kPa closely resembles that under 150 kPa normal pressure without curing stress. In the case of the specimen with a moisture content of 104.3 % and a cement content of 50 kg/m^3, the increase in the pull-out force due to curing stress was substantial, as shown in **Figure 5b**. This suggests that the effect of curing stress on the pull-out characteristics of the interface between low-cement-content stabilized slurry and the single rib of the geogrid was more pronounced.

Figure 6 presents a comparison of the peak pull-out forces with and without curing stress for specimens with varying moisture contents and cement contents, subjected to different normal stresses. Regardless of the normal stress level, applying a curing stress consistently enhanced the peak pull-out force for the samples with the same moisture content and cement content. The increase in peak pull-out force, expressed as a percentage, ranged from 8 % to 58 %. When examining the influence of moisture content, the increase rate varied between 12 % and 21 %. This indicated that higher moisture contents generally resulted in a lower percentage increase in peak pull-out force when a curing stress was applied. In contrast, the effect of cement content showed a broader range, with the increase rate spanning from 8 % to 58 %. This suggested that the application of curing stress had a more pronounced effect on the samples with lower cement contents, leading to a greater enhancement in peak pull-out force.

Furthermore, the trend observed in the data suggested that both increasing moisture content and increasing cement content tended to reduce the overall increase rate. However, the reduction in the increase rate due to cement content was more significant compared to that caused by moisture content. This implied that the interaction between cement content and curing stress played a critical role in determining the effectiveness of the curing stress in enhancing the pull-out strength.

3.2 Interfacial shear strength parameters

In the pull-out test, the interfacial strength parameters serve as critical indices for assessing the interfacial interaction between the individual rib of the geogrid and the stabilized slurry, encompassing both interfacial cohesion and the interfacial friction angle. These parameters are derived through curve fitting of the interfacial shear strength data against the normal pressure. The calculation of interfacial shear strength can be accomplished using the following equation:

$$\tau = \frac{T_{\max}}{A_{f\cdot s}} = \frac{T_{\max}}{2(a+b)l} \tag{1}$$

Here,

τ (kPa) – represents the interfacial shear strength.

$T_{\max}$ (kN) – denotes the peak pull-out force.

l (m) – signifies the effective length of the rib embedded in the stabilized slurry.

a (m) – indicates the width of the rib buried in the stabilized slurry.

b (m) – refers to the thickness of the rib.

Figure 7 illustrates the relationship between the interfacial shear strength (τ) and normal pressure (σ) for specimens under varying moisture contents and cement dosages, with and without the application of curing stress. The regression line unequivocally illustrates a linear dependence between the interfacial shear strength and the normal pressure. The trend of the shear strength increasing with the normal pressure is uniform, irrespective of whether a curing stress is applied. Upon comparing the samples with the same cement content but different moisture levels, it is observed that a lower moisture content is associated with a higher interfacial shear strength at the same normal pressure, indicating a negative correlation between the two variables. Furthermore, when considering the samples with the same moisture content but varying cement dosages, a higher cement dosage is found to be associated with an elevated interfacial shear strength under equivalent normal pressures. Specimens that were subjected to curing stress exhibit a significantly higher interfacial shear strength under identical conditions compared to those that were not treated. For instance, a sample with a moisture content of 104.3 % and a cement content of 100 kg/m^3 demonstrates an interfacial shear strength ranging from 169.40 kPa to 223.69 kPa under normal pressures of 50 kPa to 150 kPa in the absence of curing stress. After the application of curing stress, the interfacial shear strength increases to a range of 196 kPa to 250.07 kPa.

By analyzing the parameter values of the fitted line between the interfacial shear strength and the normal stress, the parameters related to the interfacial strength can be determined. Specifically, the intercept of the line represents the interfacial cohesion, while the arctangent

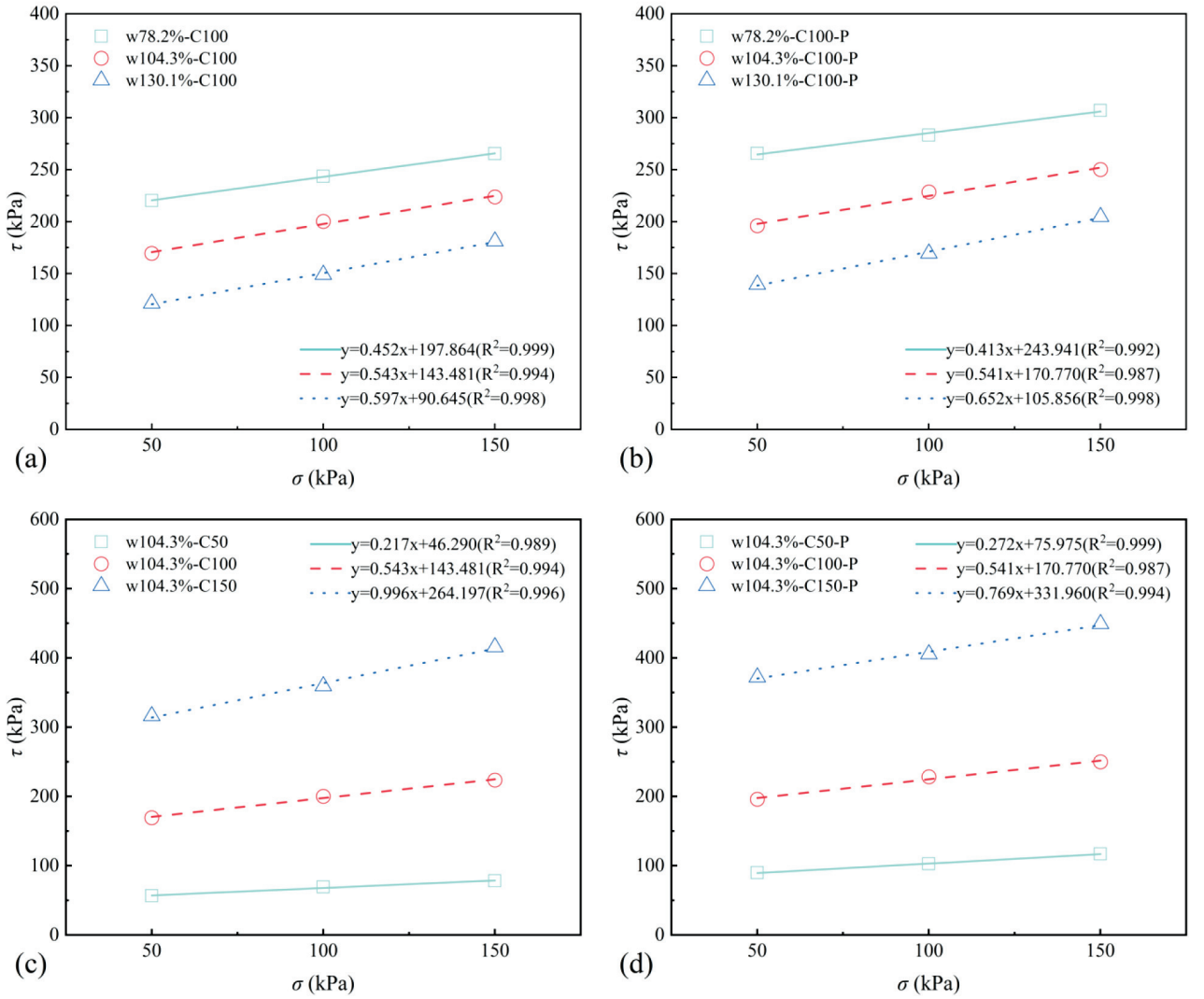

Figure 7: Interface shear strength-normal pressure relationships for specimens under varying water contents: a) without and b) with curing stress, as well as different levels of cement contents c) without and d) with curing stress

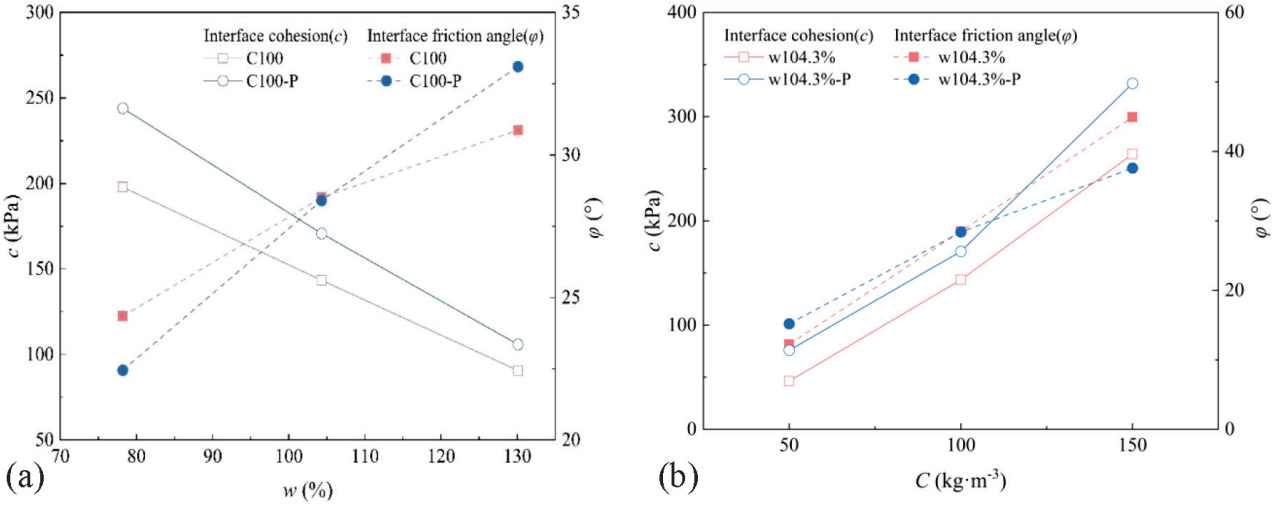

Figure 8: Relationship between interface cohesion and friction angle, influenced by: a) water content and b) cement dosage for specimens without and with curing stress

of the line's slope corresponds to the interfacial friction angle. **Table 4** presents the interfacial cohesion and friction angles of the specimens. **Figure 8** depicts the variation in interfacial cohesion and friction angle of the specimens under the influence of moisture and cement content, with and without the application of curing stress. Based on **Table 4** and **Figure 8**, it was observed that, regardless of whether curing stress was applied, interfacial cohesion decreases significantly with increasing moisture content at the same cement dosage, while the interfacial friction angle experiences a slight increase. For instance, when the cement content is 100 kg/m^3, the interfacial cohesion of the specimen without curing stress and with the moisture content increasing from 78.2 % to 130.1 % decreases from 197.86 kPa to 90.65 kPa, while the interfacial friction angle increases from 24.35° to 30.87°. For the specimens subjected to curing stress, the interfacial cohesion drops from 243.94 kPa to 105.86 kPa, and the interfacial friction angle increases from 22.45° to 33.10°. As indicated by **Figure 7**, the interfacial shear strength at a moisture content of 78.2 % is significantly higher than that at 130.1 %, suggesting that moisture content has a more profound impact on interfacial cohesion than on friction angle.

For the same moisture content, interfacial cohesion increases substantially with the increase in cement dosage, and the interfacial friction angle also shows a considerable increase. For example, when the moisture content is 104.3 %, the interfacial cohesion of the specimen without curing stress and with the cement dosage increasing from 50 kg/m^3 to 150 kg/m^3 increases from 46.29 kPa to 264.20 kPa, and the interfacial friction angle increases from 12.24° to 44.91°. For the specimens with the curing stress applied, the interfacial cohesion increases from 75.98 kPa to 331.96 kPa, and the interfacial friction angle rises from 15.2° to 37.6°. It was inferred that cement dosage simultaneously affects both interfacial cohesion and friction angle. Furthermore, by comparing the values of the specimens with the same moisture content and cement dosage, with and without curing stress, it is found that the change in the interfacial friction angle is relatively small, indicating that the curing stress primarily influences the interfacial cohesion between the geogrid single rib and the stabilized dredged slurry, rather than the friction angle.

Table 4: Comparison of interfacial cohesion and friction angle values between specimens with and without applied curing stresses

Water content (%)	Cement content (kg/m^3)	Without curing stress		With curing stress	
		c (kPa)	φ (°)	c (kPa)	φ (°)
78.2	100	197.86	24.35	243.94	22.45
104.3	50	46.29	12.24	75.98	15.20
104.3	100	143.48	28.51	170.77	28.40
104.3	150	264.20	44.91	331.96	37.60
130.1	100	90.65	30.87	105.86	33.10

4 CONCLUSIONS

Given the complex interlocking mechanism of a geogrid mesh, an accurate assessment of the effects of curing stress on cement-stabilized soil reinforced with geogrid requires a prior understanding of the interface frictional properties. This study utilized pull-out tests to investigate the interface characteristics of cement-stabilized dredged slurry reinforced with a single geogrid rib, with the mesh openings removed. The research focused on how water content, cement dosage, and curing stress influence these interface properties. The findings from the experiments led to the following conclusions:

1. The pull-out displacement curves, whether or not curing stresses were applied, demonstrated that the pull-out force increased rapidly with displacement in the initial stage and then gradually decreased after reaching the peak pull-out force. For the specimens with the same moisture content, cement dosage, and normal pressure,

and subjected to curing stress, the peak pull-out forces were consistently higher than for the specimens that had not undergone such stress.

2. The increase in the interfacial shear strength with normal pressure remained consistent, irrespective of whether the curing stress was applied. A reduced moisture content correlated with an elevated shear strength, and a higher cement dosage was associated with an increased shear strength at the same pressure levels.

3. The interfacial cohesion diminished significantly with a higher moisture content, whereas the friction angle exhibited only a slight increase. The influence of the moisture content on cohesion was more pronounced than that on friction angle. Additionally, at the same moisture level, both interfacial cohesion and friction angle rose significantly with an increased cement content. The curing stress appeared to predominantly affect the interfacial cohesion, with a relatively minor impact on the friction angle.

In this study, only one type of geogrid and one type of dredged slurry were selected, and the applicability of the results needs to be validated through a larger sample size. Future research will expand the range of samples, adopt multiple types of geogrids, consider the influence of geogrid mesh, and integrate image acquisition technology to further elucidate interfacial mechanisms.

Acknowledgment

This study was supported by the Jiangsu Provincial Basic Science (Natural Science) Research Project for Higher Education Institutions (No.25KJA560004), the Jiangsu Provincial University-Industrial Research Collaboration Project (No. BY20221035), and the Postgraduate Research & Practice Innovation Program of Yancheng Institute of Technology (No. KYCX24_XY047). It study was also sponsored by the Jiangsu Qinglan Project, which is highly appreciated.

5 REFERENCES

[1] J. Zhang, X. Wang, J. Shen, Influence of cement content and moisture content on the pullout-interface properties of geogrid-solidified waste mud, Mater. Tehnol., 57 (**2023**), 333–339, doi:10.17222/mit.2023.848

[2] Y. H. Huang, C. Dong, C. L. Zhang, K. Xu, A dredged material solidification treatment for fill soils in East China: A case history, Mar. Georesour. Geotechnol., 35 (**2017**), 865–872, doi:10.1080/1064119X.2016.1257669

[3] C. C. Qiu, G. Z. Xu, D. Zhang, F. H. Wu, D. H. Cao, Effect of curing stress on the interface property of cement-treated dredged mud and geogrid, Mar. Georesour. Geotechnol., (**2024**), doi:10.1080/1064119X.2024.2322686

[4] X. X. He, Y. J. Chen, Y. Wan, L. Liu, Q. Xue, Effect of Curing Stress on Compression Behavior of Cement-Treated Dredged Sediment, Int. J. Geomech., 20 (**2020**), 04020204, doi:10.1061/(ASCE)GM.1943-5622.0001857

[5] X. Bian, L. L. Zeng, Y. F. Deng, X. Z. Li, The role of superabsorbent polymer on strength and microstructure development in cemented dredged clay with high water content, Polymers, 10 (**2018**), 1069, doi:10.3390/polym10101069

[6] G. Z. Xu, Y. F. Gao, C. J. Xu, Permeability behavior of high-moisture content dredged slurries, Mar. Georesour. Geotechnol., 33 (**2015**), 348–355, doi:10.1080/1064119X.2014.890258

[7] X. Bian, W. H. Peng, C. C. Qiu, G. Z. Xu, Y. K. Yao, Model test on bearing capacity of cemented slurry reinforced pile composite foundation, Case Stud. Constr. Mater., 19 (**2023**), e02482, doi:10.1016/j.cscm.2023.e02482

[8] A. Maher, W. S. Douglas, F. Jafari, Field Placement and Evaluation of Stabilized Dredged Material (SDM) from the New York/New Jersey Harbor, Mar. Georesour. Geotechnol., 24 (**2006**), 251–263, doi:10.1080/10641190600788460

[9] G. Z. Xu, Q. Y. Han, Z. H. Wang, J. X. Wu, J. Yin, Eco-friendly rice straw as vertical drains for dredged slurry treatment as construction fill, Constr. Build. Mater., 345 (**2022**), 128244, doi:10.1016/j.conbuildmat.2022.128244

[10] F. Ji, J. X. Weng, M. M. Song, D. Yao, D. Zhang, Investigation on rheological and strength characteristics of cement-treated dredged materials, Mar. Georesour. Geotechnol., 40 (**2022**), 1265–1274, doi:10.1080/1064119X.2021.1992050

[11] N. Yoobanpot, P. Jamsawang, H. Poorahong, P. Jongpradist, S. Likitlersuang, Multiscale laboratory investigation of the mechanical and microstructural properties of dredged sediments stabilized with cement and fly ash, Eng. Geol., 267 (**2020**), 105491, doi:10.1016/j.enggeo.2020.105491

[12] G. Bi, S. H. Yang, Y. Wu, Y. J. Sun, H. Z. Xu, B. K. Zhu, C. X. Huang, S. Q. Cao, A preliminary study of the application of the strain-self-sensing smart geogrid rib in expansive soils, Geotext. Geomembr., 51 (**2023**), 275–281, doi:10.1016/j.geotexmem.2022.10.005

[13] M. C. Jia, W. K. Zhu, C. Xu, Performance of a 33m high geogrid reinforced soil embankment without concrete panel, Geotext. Geomembr., 49 (**2021**), 122–129, doi:10.1016/j.geotexmem.2020.07.008

[14] R. Sukkarak, P. Jongpradist, W. Kongkitkul, P. Jamsawang, S. Likitlersuang, Investigation on load-carrying capacity of geogrid-encased deep cement mixing piles, Geosynth. Int., 28 (**2021**), 450–463, doi:10.1680/jgein.21.00026

[15] J. Izawa, H. Ito, T. Saito, M. Ueno, J. Kuwano, Development of rational seismic design method for geogrid-reinforced soil wall combined with fibre-mixed soil-cement and its applications, Geosynth. Int., 16 (**2009**), 286–300, doi:10.1680/gein.2009.16.4.286

[16] M. Sugimoto, A. M. N. Alagiyawanna, K. Kadoguchi, Influence of rigid and flexible face on geogrid pullout tests, Geotext. Geomembr., 19 (**2001**), 257–277, doi:10.1016/S0266-1144(01)00011-5

[17] C. Chen, G. R. McDowell, N. H. Thom, Investigating geogrid-reinforced ballast: Experimental pull-out tests and discrete element modelling, Soils Found., 54 (**2014**), 1–11, doi:10.1016/j.sandf.2013.12.001

[18] Z. J. Wang, F. Jacobs, M. Ziegler, Experimental and DEM investigation of geogrid–soil interaction under pullout loads, Geotext. Geomembr., 44 (**2016**), 230–246, doi:10.1016/j.geotexmem.2015.11.001

[19] Z. J. Wang, Q. S. Xia, G. Q. Yang, W. Y. Zhang, G. W. Zhang, Effects of transverse members on geogrid pullout behavior considering rigid and flexible top boundaries, Geotext. Geomembr., 51 (**2023**), 72–84, doi:10.1016/j.geotexmem.2023.03.005

[20] R. J. Zhang, J. J. Zheng, X. Y. Bian, Experimental investigation on effect of curing stress on the strength of cement-stabilized clay at high water content, Acta Geotech., 12 (**2017**), 921–936, doi:10.1007/s11440-016-0511-3